$(p, 2p)$ and (p,pd) reactions on ^{3}He at 45.0 MeV†

S. N. Bunker,* Mahavir Jain,‡ C. A. Miller,§ J. M. Nelson,¶ and W. T. H. van Oers
Cyclotron Laboratory, Department of Physics, University of Manitoba, Winnipeg, Manitoba, R3T 2N2
(Received 26 June 1975)

The reactions ^{3}He$(p, 2p)d$, ^{3}He$(p, pd)p$, and ^{3}He$(p, 2p)pn$ have been studied at 45.0 MeV using a coplanar symmetric geometry. Angular correlations have been obtained for both the ^{3}He$(p, 2p)d$ and ^{3}He$(p, 2p)d^*$ reactions. Within the framework of the plane-wave impulse approximation (PWIA) the extracted momentum distributions of the $p+d$ and $p+d^*$ systems in ^{3}He are compared with predictions calculated using relatively simple wave functions for ^{3}He, d, and d^*. Reasonable agreement between the shapes of the extracted and theoretical momentum distributions has been obtained. There exist differences between the momentum distributions extracted from the angular correlation and energy-sharing data. The PWIA predictions overestimate the cross sections by appreciable factors. The ^{3}He(p, pd) quasifree scattering enhancements exhibit shifts in the peak position away from the minimum in the momentum of the spectator proton. The ^{3}He$(p, 2p)pn$ continua are to first approximation in agreement with differential phase-space distribution predictions if the kinematic region of low energy for the relative motion of the unobserved n-p pair is excluded.

[NUCLEAR REACTIONS ^{3}He$(p,2p)^2$H, ^{3}He$(p,2p)pn$, ^{3}He$(p,pd)^1$H, T_1=45.0 MeV; measured $d\sigma/(dT_3 d\Omega_3 d\Omega_4)$ in coplanar geometry; deduced momentum distributions using PWIA; compared with theoretical momentum distributions; investigated four-body continua.]

I. INTRODUCTION

The analysis of $(p, 2p)$ quasifree scattering experiments in the plane-wave (PWIA) or distorted-wave (DWIA) impulse approximation has provided valuable nuclear structure information.[1] At higher energies, i.e., above 100 MeV, the $(p, 2p)$ reaction is fairly well described as the direct interaction between the incident and struck protons, which facilitates the extraction of single-particle properties of the target nucleus. It has also become apparent that the interpretation of quasifree scattering data at lower energies becomes more difficult owing to the increased complexity of the reaction mechanism, multiple scattering, and the presence of off-energy-shell effects.[2] Within the framework of PWIA and DWIA treatments of knock-out reactions the analysis of the data is facilitated by the factorization of the three-body cross section. A comparison of the ^{3}He$(p, 2p)d$ and ^{3}He$(p, pd)p$ reactions gives a test on the validity of factorization provided a high enough incident proton energy is chosen. In the PWIA the differential cross section can be expressed as

$$\frac{d\sigma}{d\Omega_3 d\Omega_4 dT_3} = F\left(\frac{d\sigma}{d\Omega}\right)^{p-x} N\,|\,\phi(\vec{q}=-\vec{p}_5)\,|^2 ,$$

where F is essentially the differential phase-space distribution factor, $(d\sigma/d\Omega)^{p-x}$ is the two-body cross section for the interaction of the incident proton with the struck particle x, N is a factor due to spin summation and antisymmetrization, and $|\phi(\vec{q}=-\vec{p}_5)|^2$ is the square of the Fourier transform of the overlap integral between the spatial wave functions of the target nucleus and the residual nucleus. In the notation adopted T_i and $\vec{p}_i$ $(i=1-5)$ refer to the laboratory kinetic energy and three-momentum of the incident proton, the target nucleus, the observed particles in the element of solid angle $d\Omega_3$ and $d\Omega_4$, respectively, and the spectator particle. Usually $(d\sigma/d\Omega)^{p-x}$, which properly is the square of a half-off-energy-shell scattering amplitude, is replaced by the free p-x differential cross section evaluated at the center-of-mass energy of the two interacting particles either in the initial state or in the final state. The factor N equals $\frac{3}{2}$ for the He$(p, 2p)d$ reaction, $\frac{1}{2}$ for the ^{3}He$(p, 2p)d^*$ reaction, and $\frac{3}{2}$ for the ^{3}He$(p, pd)p$ reaction. Here, d^* refers to an n-p pair in a $^1S_0$ state with low energy for their relative motion. It should be noted that the integral $\int |\phi(\vec{q})|^2 d^3q$ is generally less than 1 since the target-nucleus wave function does not factor into a unique residual nucleus. A general conclusion[3] from PWIA analyses of $(p, 2p)$ reactions on the very light nuclei has been that the behavior of the quasifree scattering peak is extremely sensitive to the asymptotic form of the overlap function in coordinate space and that although the PWIA can give good general agreement with the shape and position of the experimentally observed peak when

overlap functions with appropriate tails are used, theory predicts cross sections larger than experiment. This discrepancy slowly decreases with increasing incident proton energy and is strongly dependent on the mass of the target particle. In addition there are deviations between the momentum distributions extracted from experiment and the theoretical ones for large momenta ($q > 100$ MeV/c), which cannot be explained within the framework of the PWIA.

Previously, the ^{3}He$(p, 2p)d$ reaction has been studied at 35 MeV by Šlaus *et al.*[4] at 65, 85, and 100 MeV by Pugh *et al.*,[5] at 155 MeV by Frascaria *et al.*[6] and at 590 MeV by Kitching *et al.*[7] The data consist of angular correlation and/or energy-sharing data. Theoretical momentum distributions for the $p+d$ system in an S-state relative motion calculated from the overlap of Irving-Gunn and Hulthén wave functions for ^{3}He and d, respectively, are in general somewhat broader than the distributions extracted from experiment. The inclusion of a 1 to 2% S'-state admixture to the ground state of ^{3}He has been considered by Frascaria *et al.*[6] These authors found a 10% increase in the cross section for a 2% S'-state admixture. These authors also included the effects of distortion in the initial and final states resulting in better agreement with experiment. It should be noted that the experiment at 590 MeV, because of the experimental energy resolution, was unable to distinguish between $(p, 2p)$ events from the ^{3}He$(p, 2p)d$ and ^{3}He$(p, 2p)d^*$ reactions.

A momentum distribution for the $p+d^*$ system in ^{3}He was obtained previously at 155 MeV.[6] The ratio of the peak cross sections of the ^{3}He$(p, 2p)d$ and ^{3}He$(p, 2p)d^*$ reactions at 35 MeV is estimated to be about 10, when energies for the relative motion of the n-p pair between 0 and 1.8 MeV are included.[8] The ratio of the maxima of the cross sections at 155 MeV is almost 4.5. However, it should be noted that quite a large fraction of the ^{3}He$(p, 2p)np$ continuum was included in determining the ^{3}He$(p, 2p)d^*$ cross sections at this energy. When a restriction is made to energies of the relative motion of the spectator $n-p$ less than 6 MeV, which because of the energy resolution corresponds to essentially the same ^{3}He$(p, 2p)d^*$ band, then the ratio becomes about 5.9.

A comparison of the ^{3}He$(p, 2p)d$ and ^{3}He$(p, pd)p$ reactions at 65, 85, and 100 MeV, using geometries which allow zero spectator momentum, indicates that the ratio of the cross sections for the two reactions is in agreement with that predicted by PWIA.[9] At 156 MeV the experimental cross sections for the two reactions are well accounted for by DWIA calculations.[10]

Studies of the ^{3}He$(p, 2p)np$ continua were made at 35 MeV and the differential cross sections were compared with four-body differential phase space distributions.[11] Several deviations from the phase-space distributions were observed.

II. EXPERIMENTAL PROCEDURE

The experiment was performed with a momentum analyzed proton beam from the University of Manitoba sector focused cyclotron. The incident proton energy was 45.0 ± 0.2 MeV while the beam energy spread was approximately 300 keV full width at half maximum (FWHM). The target was gaseous ^{3}He of 99.5% purity which was contained in a 6 cm diameter gas cell covered with a 0.025 mm thick Kapton-H foil. The gas pressures were always chosen to be slightly larger than one atmosphere and were read with a precision pressure gauge to an accuracy of ± 0.05 psi. The gas cell was flushed regularly to prevent buildup of contaminations. Two detector telescopes with closely similar geometries and each consisting of a 200 μm thick ΔE surface barrier detector, a 5 mm lithium-drifted silicon E detector, and a 500 μm veto detector viewed the target. The gas-scattering geometry was defined by two pairs of collimators with rectangular apertures. The aperture dimensions (width$\times$height in mm) were 3.18×11.1 and 6.35×9.14. The collimators were positioned at 4.45 and 11.43 cm from the center of the gas cell. The corresponding polar angle subtended by each of the double-aperture systems as defined by the width at half value of the efficiency function was $\Delta\theta \sim 2.8°$. The cross section of the incident beam at the center of the gas cell was typically 3 mm wide by 8 mm high. Beam currents up to 50 nA were used, depending on the angles. The incident proton beam was captured in a well-shielded Faraday cup. The beam current was integrated using a standard current indicator-integrator. Two monitor counters with closely similar geometries set at equal angles (37.5°) left and right with respect to the incident beam were used to check that the incident beam direction coincided with the zero-degree axis of the scattering chamber. Viewing a thin solid target (nickel), it was required that the ratio of elastically scattered protons observed by the two monitor detectors be equal to 1.00 ± 0.02. Slight adjustments in the beam transport parameters were made until this requirement was met. Checks were made repeatedly during the course of the experiment.

Using standard electronics, a timing resolution within the 35 nsec separation of cyclotron beam bursts was obtained. For each telescope high-energy protons were rejected by the veto detectors, and events that produced pulses occurring within

4 μsec from each other were eliminated by pileup gates on the ΔE signals. In most of the runs, the data were also stored in 64×64 arrays for inspection during data collection. Real and accidental spectra for both the $(p,2p)$ and (p,pd) reactions were obtained. Data were taken at the symmetric coplanar angles $\theta_3=\theta_4=25°$, 30°, 35°, 37.4°, 40°, 45°, 50°, and 60°, $\phi_{34}=180°$. The energy calibration for the T_3 and T_4 axes was obtained with an uncertainty of ±150 keV from coincident p-p elastic scattering events. The over-all energy resolution of the correlated energy spectra was about 600 keV (FWHM) along the diagonal in the T_3-T_4 plane. This gave complete separation between the bands of the ^{3}He$(p,2p)d$ and ^{3}He$(p,2p)d^*$ reactions.

For analysis, the data recorded with 1024×1024 channel resolution were used. Particle identification to separate proton-proton from proton-deuteron events was performed numerically. The resulting two-dimensional energy spectra show prominent bands due to the ^{3}He$(p,pd)p$ reaction and the ^{3}He$(p,2p)d$ and ^{3}He$(p,2p)d^*$ reactions. The latter forms the boundary of the four-body continuum from the ^{3}He$(p,2p)np$ reaction. Projections onto the energy axes were obtained by drawing bands enclosing the events of interest corresponding to the three reactions. The counts within these bands (which had approximately the same width for all angle pairs) were summed for a given energy channel. For the ^{3}He$(p,2p)d^*$ reaction at $\theta_3=\theta_4=40°$, the width of the projection band corresponded to the n-p pair having energies for their relative motion from 0 to 2.2 MeV. The projected cross sections $d\sigma/(dT_3 d\Omega_3 d\Omega_4)$ were corrected for accidental coincidences and losses from pileup rejection. The cross sections are shown in Figs. 1, 2, and 3, respectively. Note that particle identification required ΔE and E signals from each detector telescope so that there are experimental cutoffs in the energy sharing spectra, which are slightly in excess of the maximum energies which can be deposited by protons or deuterons in 200 μm of silicon (5.0 and 6.5 MeV, respectively). The error bars on the data points include statistical errors only. An estimate of the relative error (±6%) of the projected cross sections was calculated by comparing the data for four angle pairs taken in two different experimental runs. The absolute cross sections are accurate to better than 10%. The main contribution to the absolute error stems from the uncertainties in the calculation of the gas geometry factor for coincidence experiments.

III. RESULTS

A. ^{3}He$(p,2p)d$ and ^{3}He$(p,2p)d^*$

Comparison of Figs. 1 and 2 shows the strong similarity between the ^{3}He$(p,2p)d$ and ^{3}He$(p,2p)d^*$

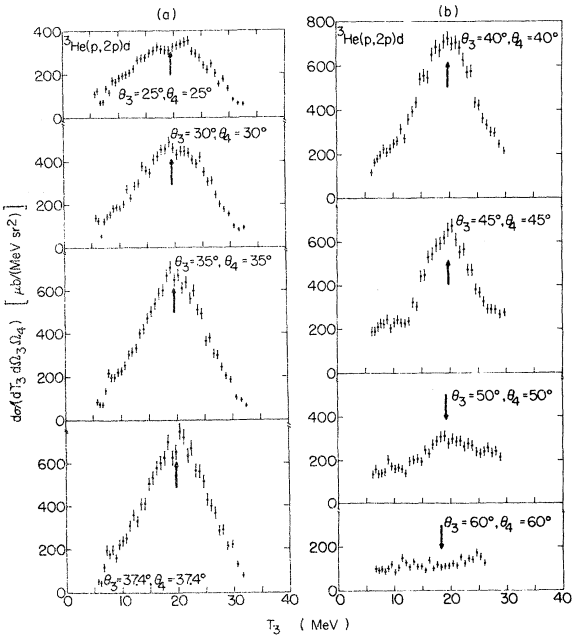

FIG. 1. Energy-sharing spectra of the ^{3}He$(p,2p)d$ reaction at 45.0 MeV. (a) Symmetric coplanar angles $\theta_3=\theta_4=25°$, 30°, 35°, and 37.4°. (b) Symmetric coplanar angles $\theta_3=\theta_4=40°$, 45°, 50°, and 60°.

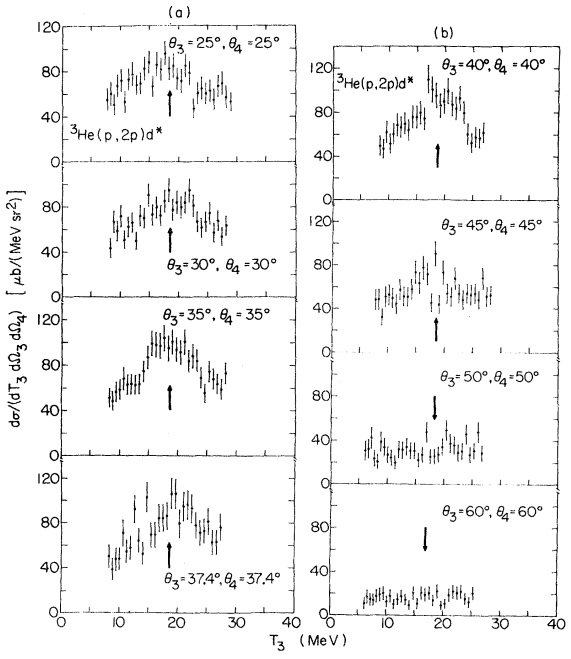

FIG. 2. Energy-sharing spectra of the ^{3}He$(p,2p)d^*$ reaction at 45.0 MeV. (a) Symmetric coplanar angles $\theta_3=\theta_4=25°$, 30°, 35°, and 37.4°; (b) Symmetric coplanar angles $\theta_3=\theta_4=40°$, 45°, 50°, and 60°.

energy sharing spectra.[13] The pronounced peaking of the energy sharing spectra disappears for angle pairs $\theta_3 = \theta_4 \geq 50°$. Furthermore, in the case of the ^{3}He$(p, 2p)d^*$ reaction there remains a structureless spectrum relatively large in magnitude at angles not close to those where zero spectator momentum is kinematically allowed. The minimum in the momentum of the spectator particle or cluster of particles is indicated in each of the spectra by an arrow in Figs. 1 to 3.

For the ^{3}He$(p, 2p)np$ reaction the relative magnitudes of the continuum and the enhancement along the boundary [which is due to the ^{3}He$(p, 2p)d^*$ reaction] appear to be quite different from what is observed for the ^{3}H$(p, 2p)nn$ reaction at 45.6 MeV.[14] This observation follows directly from a comparison of the differential cross sections $d\sigma/(dM_{56}d\Omega_3 d\Omega_4)$ for the two reactions as a function of the invariant mass M_{56} of the two unobserved particles at $\theta_3 = \theta_4 = 37.4°$. For the ^{3}He$(p, 2p)np$ reaction the relative magnitude of the continuum is approximately two times larger than for the ^{3}H$(p, 2p)$-nn reaction. It should be remarked that the unobserved np pair with low energy for the relative motion can be in a $^1S_0$ state as well as in a $^3S_1$ state. However, along the boundary of the continuum and with $T_3 \sim T_4$ the contribution to the cross section of the ^{3}He$(p, 2p)np$ reaction with the np pair in a $^3S_1$ state is small compared to the contribution of the

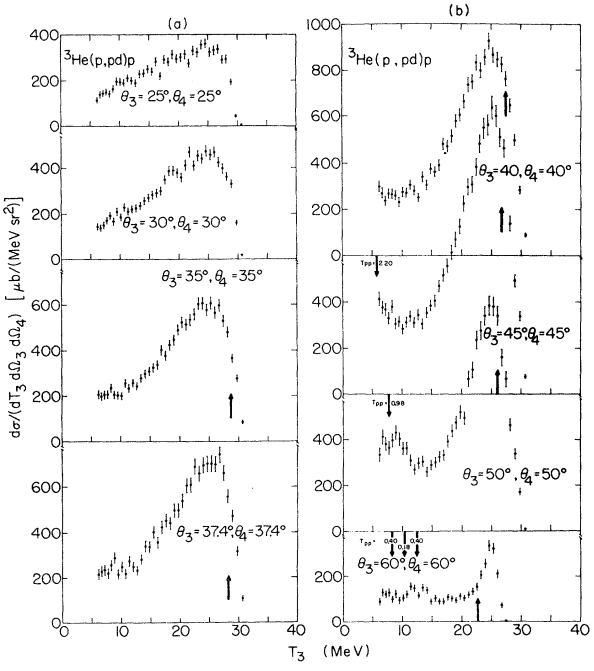

FIG. 3. Energy-sharing spectra of the ^{3}He$(p, pd)p$ reaction at 45.0 MeV. (a) Symmetric coplanar angles $\theta_3 = \theta_4 = 25°$, 30°, 35°, and 37.4°; (b) Symmetric coplanar angles $\theta_3 = \theta_4 = 40°$, 45°, 50°, and 60°.

^{3}He$(p, 2p)d^*$ reaction[14]. It has been neglected in the analysis of the present data.

The projected cross sections at approximately equal energies $T_3 = T_4$ were averaged over increasing intervals of 1.4 to 4.9 MeV in T_3 as the minimum spectator momentum $|\vec{p}_5 = -\vec{q}|$ increased from 0 to 108 MeV/c. The resulting angular correlation data for the ^{3}He$(p, 2p)d$ and ^{3}He$(p, 2p)d^*$ reactions are given in Fig. 4. The error bars include the statistical error and an estimate of the relative error (±6%) of the projected cross sections. The two angular correlations have similar characteristics except for a small shift due to the fact that zero spectator momentum for the ^{3}He$(p, 2p)$ reaction occurs at the symmetric angle pair 38.5°-38.5°. Also it is seen that the ^{3}He$(p, 2p)d^*$ reaction cross section remains high at low symmetric angles. The ratio of the peak cross sections for the ^{3}He$(p, 2p)d$ and ^{3}He$(p, 2p)d^*$ reactions at 45.0 MeV is 7.2 and is intermediate to a ratio of about 10 at 35 MeV and a ratio of 5.9 at 155 MeV. This tends

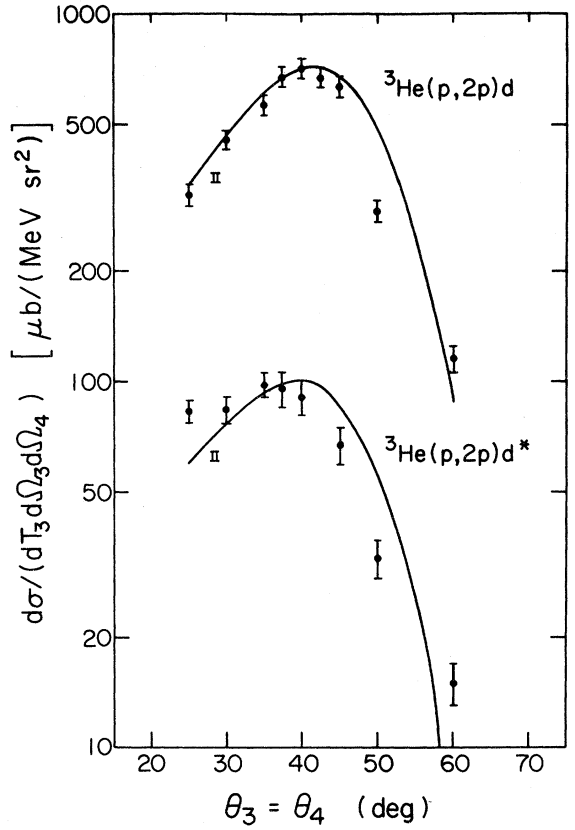

FIG. 4. Angular correlations for the ^{3}He$(p, 2p)d$ and ^{3}He$(p, 2p)d^*$ reactions at 45.0 MeV. The solid lines correspond to PWIA predictions calculated using the final-state prescription and an overlap integral containing a Hulthén wave function for the deuteron and a variational wave function for ^{3}He.

to confirm that the observed ratio increases for decreasing energy. This might be explained as resulting from the larger binding energy of a d^* system compared to a deuteron in ^{3}He which has the effect of reducing the long range part of the relative motion wave function. Absorption has the effect of localizing the quasifree scattering reaction near the nuclear surface. Its relative importance decreases with increasing energy. Consequently the above ratio for the cross sections should increase with decreasing incident energy.

The analysis of the data was performed using the PWIA. The square of the half-off-energy-shell p-p scattering amplitude was approximated by the free p-p scattering differential cross section at the appropriate c.m. energy of the p-p system in the initial and final state, respectively. The values for $(d\sigma/d\Omega)^{p-p}$ were obtained by interpolation from published cross sections.[15] The appropriate c.m. angle for the symmetric coplanar case is 90°. The quantities $N|\phi(\vec{q})|^2$ extracted from the angular correlation data for the $p+d$ and $p+d^*$ systems using both the initial and final state prescriptions are shown in Fig. 5. In this and the following figures the quantity $q=|\vec{q}|$ has been arbitrarily assigned a positive or negative value if the spectator (particle 5) is emitted parallel or antiparallel to the direction of the incident particle or on the same or opposite side as particle 3. Qualitatively the extracted $|\phi(\vec{q})|^2$ show the expected distributions due to the knockout of an s-state proton. The initial and final state prescriptions predict quite similar shapes. It has been argued that the initial state prescription provides a much better approximation to the square of the exact half-off-energy-shell p-p scattering amplitude than the final state prescription.[16] Assuming the $|\phi(\vec{q})|^2$ to be the

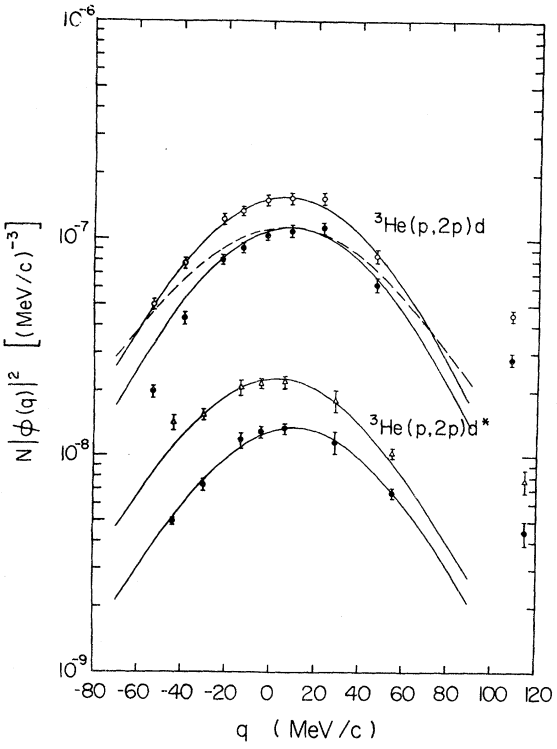

FIG. 5. Momentum distributions for a $p+d$ system and $p+d^*$ system, respectively, in ^{3}He extracted from the ^{3}He$(p,2p)$ angular-correlation data in the framework of the PWIA and using both the initial-state and final-state prescriptions. The curves correspond to theoretical momentum distributions normalized to the experimental ones at the peak values: for the ^{3}He$(p,2p)d$ reaction using no cutoff (dashed line) and using a cutoff radius of 2.5 fm (solid lines) in the overlap integral of a Hulthén wave function for the deuteron and an Irving-Gunn wave function for ^{3}He; for the ^{3}He$(p,2p)d^*$ reaction calculated using an overlap integral containing a zero-energy scattering-state wave function for d^* and an Irving-Gunn wave function for ^{3}He. Note the shifts from zero spectator momentum in the theoretical distributions. The Irving-Gunn wave function has $\alpha=0.770$ fm^{-1}.

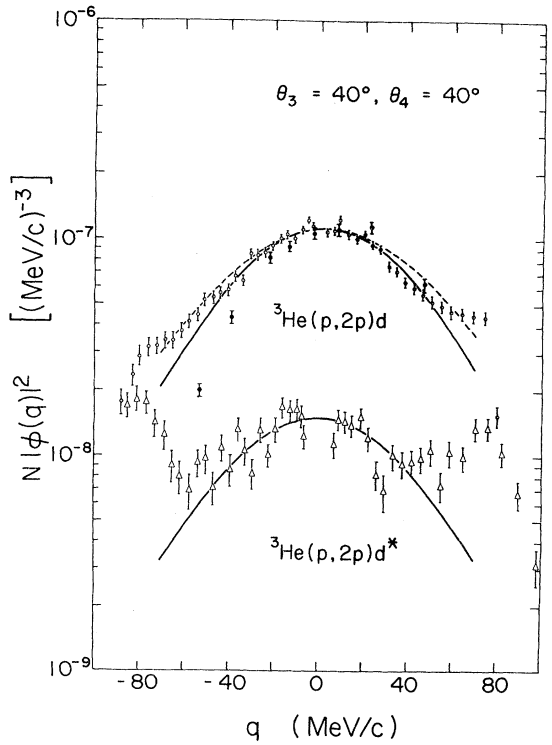

FIG. 6. Momentum distribution for a $p+d$ and a $p+d^*$ system, respectively, in ^{3}He extracted from the ^{3}He$(p,2p)$ energy-sharing data at $\theta_3=\theta_4=40°$ in the framework of the PWIA and using the final-state prescription. For ^{3}He$(p,2p)d$ comparison is made with the corresponding quantities $N|\phi(\vec{q})|^2$ extracted from the angular-correlation data. Also shown are the theoretical momentum distributions of Fig. 5.

same for the $p+d$ and $p+d^*$ systems in ^{3}He, the ratio of the quantities $N|\phi(q)|^2$ shown in Fig. 5 should be $\frac{3}{2}$ to $\frac{1}{2}$. The ratio of the peaks of the momentum distributions for the $p+d$ and $p+d^*$ systems is 6.7. Furthermore, the peaks are shifted by approximately 6 and 3 MeV/c from zero spectator momentum, respectively, when the initial state prescription is used and by 8 and 10 MeV/c, respectively, when the final state prescription is used. Such shifts have been interpreted as resulting from distortion and/or refraction effects.[17,18]

In principle the energy sharing spectrum obtained at the pair of symmetric scattering angles for which the spectator momentum reaches the value zero should lead to an identical momentum distribution. The quantities $N|\phi(\vec{q})|^2$ extracted from the energy sharing spectra at 40°-40° using the final state prescription are shown in Fig. 6. For the ^{3}He$(p, 2p)d$ reaction they are compared with the quantities $N|\phi(\vec{q})|^2$ extracted from the angular correlation data. There is reasonable agreement although the momentum distribution extracted from the energy sharing data appears to be somewhat wider than the one extracted from the angular correlation data. The momentum distribution extracted from the energy sharing data is, as it should be, symmetric about zero spectator momentum; however, the momentum distribution extracted from the angular correlation data appears shifted by approximately 8 MeV/c. It should be noted that since the low and high energy ends of the 40°-40° ^{3}He$(p, 2p)d$ energy-sharing spectrum (large values of $|\vec{q}|$) correspond to low relative energies for a p-d system, at the end points less than 2 MeV, appreciable distortions may occur. Consequently, the extraction of detailed momentum distributions using the PWIA from energy-sharing data alone may be unreliable for low-energy incident protons. The rise in the momentum distribution extracted from the 40°-40° ^{3}He$(p, 2p)d^*$ energy-sharing spectrum for large values of $|\vec{q}|$ again may be attributed to the low energy between one of the observed protons and the unobserved n-p pair.

The theoretical momentum distribution for the $p+d$ system in an S-state relative motion was calculated from the overlap integral of an Irving-Gunn wave function for ^{3}He [19] and a Hulthén wave function for the deuteron.[20] The resulting distribution has a half width at half maximum (HWHM) of 52 MeV/c and is slightly wider than the momentum distribution extracted from the angular correlation data using either the initial-state or the final-state prescription. The latter momentum distribution has a HWHM of 45 ± 3 MeV/c. The theoretical momentum distribution agrees better with the one extracted from the 40°-40° energy-sharing data which has a HWHM of 48 ± 3 MeV/c. It is also interesting to note that Cowley *et al.*[9] find good agreement between the theoretical momentum distributions, calculated as the Fourier transform of an overlap integral containing the same wave functions as in the present analysis, and the momentum distributions extracted from the energy sharing data at symmetric angle pairs containing zero spectator momentum at incident proton energies of 65, 85, and 100 MeV. Frascaria *et al.*[6] find again that the PWIA cross sections have a somewhat wider distribution than the experimentally measured angular correlation at 155 MeV. Thus it appears that the PWIA calculations containing the Fourier transform of the overlap integral of an Irving-Gunn wave function and Hulthén wave function are in reasonable agreement with the energy sharing data at symmetric angle pairs for which zero spectator momentum is kinematically allowed but agree less with angular correlation data.

The PWIA calculations predict cross sections which are too large. Thus the theoretical momentum distribution has to be multiplied with a normalization factor less than one in order that the peak value agrees with the one of the momentum distribution extracted from the angular correlation data. For the final state prescription the normalization factor is $N_n = 0.169 \pm 0.017$. This value is in fair agreement with the trend as function of energy established by higher energy data.[4-7,9] (See Fig. 7.)

In order to obtain agreement between the shapes of the theoretical and experimental momentum distributions, it was found necessary to introduce a cutoff radius in the wave function for the relative motion of the p-d system, which phenomenologically takes account of multiple scattering or absorption processes. Physically this truncation implies that the quasifree scattering process occurs near

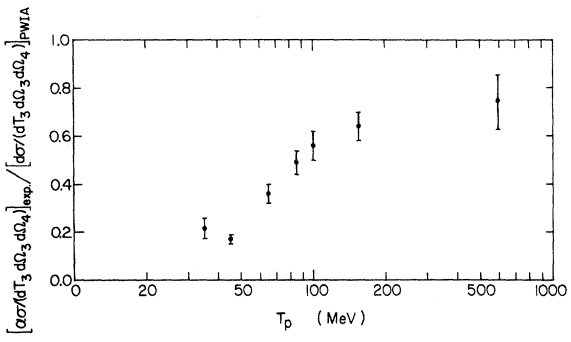

FIG. 7. Ratio of the experimental ^{3}He$(p, 2p)d$ cross sections to the PWIA cross sections for zero momentum of the spectator particle in a symmetric coplanar geometry as a function of incident-proton energy.

the nuclear surface.[17,18] The shape of the theoretical $N|\phi(q)|^2$ distribution calculated with a cutoff radius of 2.5 fm is in good agreement with the $N|\phi(\vec{q})|^2$ distribution extracted from the angular correlation data if the 60°-60° point ($q = 128$ MeV/c) is excluded (Fig. 5). For the final-state prescription the normalization factor in this case is $N_n = 0.261 \pm 0.026$. It should be pointed out that the ^{3}He ground-state wave function contains a 4–7% D-state admixture in addition to a 1–2% S'-state admixture. This D-state admixture will result in an increase in $|\phi(\vec{q})|^2$ relative to a pure S-state distribution for large values of $|\vec{q}|$. (The D-state relative-motion wave function goes to zero for $\vec{q} = 0$ and, therefore, the shape of the distribution for small values of $|\vec{q}|$ is governed by the S-state distribution). However, the observed discrepancy for the 60°-60° point is too large to be explained by the D-state admixture in ^{3}He as follows from an evaluation of similar D-state admixture effects on the momentum distribution of the deuteron.[21] It is very probably caused by multiple-scattering processes.

The ^{3}He$(p, 2p)d^*$ energy-sharing data were obtained by projecting a band corresponding to $T_{pn} \leq 2.2$ MeV or $m_5 + m_6 \leq M_{56} \leq m_5 + m_6 + \Delta (\Delta = 2.2$ MeV) onto the T_3 axis. The four-body phase-space distribution[22] increases with increasing M_{56} from $M_{56} = m_5 + m_6$:

$$\frac{dR_4(\vec{P}, E)}{dE_3 d\Omega_3 dE_4 d\Omega_4} = \tfrac{1}{4} p_3 p_4 R_2(0, M_{56}),$$

$$R_2(0, M_{56}) = \frac{\pi}{M_{56}} \frac{\{[M_{56}^2 - (m_5^2 + m_6^2)]^2 - 4m_5^2 m_5^2\}^{1/2}}{2M_{56}}.$$

To obtain the projection onto the E_3 (or T_3) axis one integrates over a range of E_4 (or T_4) values determined by the limits on M_{56}

$$\frac{dR_4(\vec{P}, E)}{dE_3 d\Omega_3 d\Omega_4} = \int_{E_4'}^{E_4''} \tfrac{1}{4} p_3 p_4 R_2(0, M_{56}) dE_4 .$$

For small Δ this can be approximated by

$$\frac{dR_4(\vec{P}, E)}{dE_3 d\Omega_3 d\Omega_4} = \frac{dR_3(\vec{P}, E)}{dE_3 d\Omega_3 d\Omega_4} (2M_{56}) R_2(0, M_{56}),$$

where $dR_3/(dE_3 d\Omega_3 d\Omega_3)$ is the three-body phase-space distribution for a system of three particles with masses m_3 and m_4, and $M_{56} = m_5 + m_6 + \frac{1}{2}\Delta$. Accordingly, the analysis of the ^{3}He$(p, 2p)d^*$ reaction was done in a manner similar to the analysis of a three-body final-state reaction.

The theoretical momentum distribution for the $p + d^*$ system in an S-state relative motion was calculated from the overlap integral of an Irving-Gunn wave function for ^{3}He and a zero-energy scattering wave function[23] for the d^* system, i.e.,

$$\psi_{d^*}(\rho) = -a_s[1 - \rho/a_s - \exp(-\xi\rho)]/\rho ,$$

$$a_s = 23.71 \text{ fm},$$

and

$$\xi = 1.14 \text{ fm}^{-1}.$$

The exponential term ensures proper behavior of the d^* wave function as $\rho \to 0$. The resulting $|\phi(\vec{q})|^2$ (with a HWHM = 45 MeV/c) fits the shape of the experimental distribution extracted from the ^{3}He-$(p, 2p)d^*$ angular-correlation data rather well (Fig. 5). No cutoff radius was introduced in this case. The same $N|\phi(\vec{q})|^2$ distribution also agrees reasonably well with the central portion of the $N|\phi(\vec{q})|^2$ distribution extracted from the 40°-40° ^{3}He$(p, 2p)d^*$ energy-sharing data (Fig. 6).

In order to investigate whether an improved ^{3}He wave function would give better agreement with experiment, PWIA calculations were made with an overlap integral in which the Irving-Gunn wave function was replaced by variational wave functions.[24] These wave functions were obtained by solving the ground state of the three-nucleon system for the Hamada-Johnston potential using a variational method. In the present calculations two wave functions were used: wave function I gave a binding energy for ^{3}He of 6.1 MeV, while wave function II gave a binding energy at 4.0 MeV. The PWIA calculations overestimate the cross sections (because of the neglect of multiple-scattering effects) and thus the theoretical angular correlations were normalized to the peak values of the experimental ones. The resulting angular correlations for wave function II are shown in Fig. 4. The normalization factor using with wave function II to obtain agreement at the peak value of the ^{3}He-$(p, 2p)d$ angular correlation was $N_n = 0.19$. Since wave function II underestimates the binding energy of ^{3}He by 3.7 MeV it has less high-momentum components in the relative-motion wave function than wave function I. It provides a more reasonable agreement with experiment.

B. ^{3}He$(p, pd)p$

One should note (Fig. 3) that the peak positions in the ^{3}He$(p, pd)p$ spectra do not correspond to the minimum value of the spectator momentum. The shift in the peak position becomes more pronounced further away from the angle pair where zero spectator momentum is kinematically allowed and amount to as much as 3 MeV for the 35°-35° spectrum. The occurrence of such shifts was observed earlier in the 35 MeV ^{3}He$(p, pd)p$ data.[4] It was conjectured that the ^{3}He$(p, d)[pp]$ neutron pickup reaction interferes strongly with the quasifree scatter-

ing process and reaches a maximum at supplementary angles for the pseudo two-body reaction $p + {}^3\mathrm{He} \rightarrow d + [pp]$, where $[pp]$ denotes a p-p pair in a $^1S_0$ state with near zero relative energy ($T_{pp} = 0.40$ MeV).[12] The importance of this pseudo two-body reaction is demonstrated by the relative increase in the cross section towards lower proton energies in the lower half of each of the 45°-45°, 50°-50°, and 60°-60° ^{3}He$(p, pd)p$ energy sharing spectra. The pair of symmetric supplementary angles for the $p + {}^3\mathrm{He} \rightarrow d + [pp]$ reaction at 45.0 MeV is $\theta_d = \theta_{[pp]} = 57.2°$. Owing to the Coulomb repulsion between the two protons the energy-sharing spectrum at this pair of angles should exhibit a double peak with a minimum at $T_{pp} = 0$ and maxima at $T_{pp} \simeq 0.40$ MeV in addition to the ^{3}He$(p, pd)p$ quasifree scattering peak. The position of the minimum value of T_{pp} is indicated in the 45°-45°, 50°-50°, and 60°-60° energy sharing spectra. Note that the angular distribution of the ^{3}He$(p, d)[pp]$ reaction at 45.0 MeV has a second maximum at $\theta_d \simeq 35°$ and decreases rapidly for increasing scattering angle.[25] One expects the interference between quasifree scattering and the neutron pickup reaction to be of particular importance for low incident energies and to disappear slowly with increasing energy owing to kinematical separation provided not too small angles are chosen.

Quantitatively this is demonstrated in Fig. 8, which exhibits momentum distributions extracted from the ^{3}He$(p, pd)p$ data using the PWIA. The four-momentum distributions were obtained from the symmetric coplanar ^{3}He$(p, pd)p$ energy-sharing spectra by selecting the two kinematical situations of $T_3 = T_4$ (the observed proton and deuteron have equal kinetic energies) and $\vec{p}_5 \| \vec{p}_1$ (the spectator momentum is collinear with the momentum of the incident proton) and applying the initial- and final-state prescriptions. These kinematical situations were chosen because they correspond to cross sections on the left-hand side of the peaks. The positions of minimum spectator momentum are close to the kinematical end points of the spectra where there is appreciable phase-space enhancement. The differential cross sections were averaged over bins 2.8 MeV wide in T_3. The square of the half-off-energy-shell p-d scattering amplitude was approximated by the free p-d differential cross section at the initial-state and final-state p-d c.m. energies, respectively, and the appropriate c.m. scattering angle. The values for $(d\sigma/d\Omega)^{p-d}$ were obtained by interpolation from published cross sections.[26] Although the $N|\phi(\vec{q})|^2$ distributions are not complete, it is apparent that after renormalization to a common value at a certain q there are differences in both the widths of the distributions and in the shifts from zero spectator momentum.

The pair of symmetric coplanar angles at which zero spectator momentum is kinematically allowed is 48.9°-48.9°. Thus one expects the shift of the quasifree scattering peak from the minimum spectator momentum to be minimal close to this pair of angles. Figure 9 displays the $N|\phi(\vec{q})|^2$ distribu-

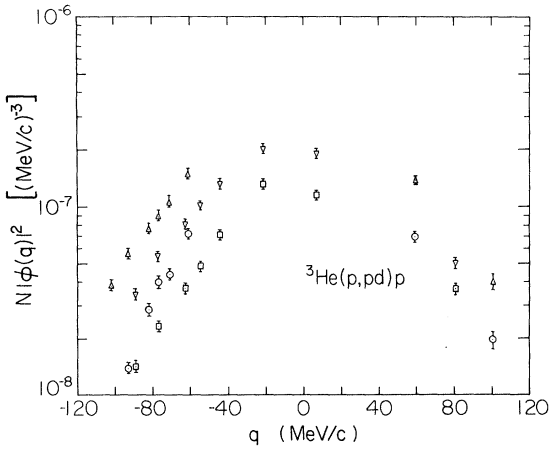

FIG. 8. Momentum distributions for a $p + d$ system in ^{3}He extracted from the ^{3}He$(p, pd)p$ data in the framework of the PWIA and using both the initial- and final-state prescriptions. Two kinematical conditions were chosen: $T_3 = T_4$, upright triangles and open circles, respectively; and $\vec{p}_5 \| \vec{p}_1$, inverted triangles and open squares, respectively.

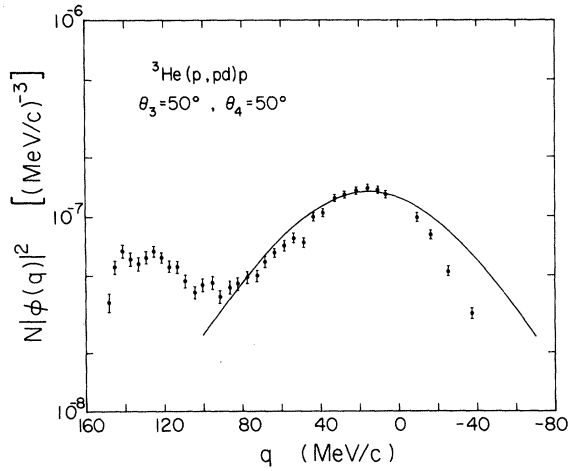

FIG. 9. Momentum distribution for a $p + d$ system in ^{3}He extracted from the ^{3}He$(p, pd)p$ 50°-50° energy-sharing data. The solid curve corresponds to the theoretical momentum distribution calculated from the overlap integral (with no cutoff) of a Hulthén wave function for the deuteron and an Irving-Gunn wave function for ^{3}He also shown in Figs. 5 and 6. Note the shift from zero momentum in the theoretical distribution.

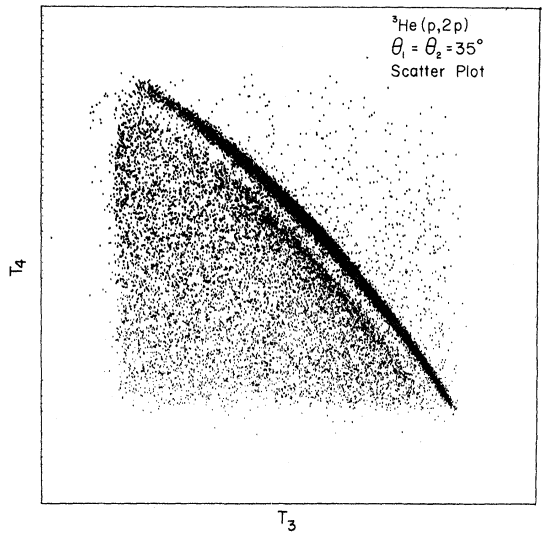

FIG. 10. Scatter plot of the ^{3}He$(p, 2p)$ reaction at 45.0 MeV and symmetric coplanar angles $\theta_3 = \theta_4 = 35°$.

tion extracted from the 50°-50° energy sharing spectrum using the final-state prescription. The rise towards large positive values of q might be due to the contribution of the ^{3}He$(p, d)[pp]$ reaction discussed above. The momentum distribution is shifted from zero spectator momentum by about 15 MeV/c. This is quite similar to what was observed by Cowley *et al.*[9] for the momentum distributions extracted from the energy-sharing data with $\theta_3 = 62.8°$, $\theta_4 = 41.8°$ at 65 MeV. The theoretical $N|\phi(q)|^2$ distribution with a HWHM of 52 MeV/c is the same as shown in Fig. 5. It is somewhat wider than the experimental distribution. The normalization constant with which the PWIA cross sections have to be multiplied to obtain agreement with experiment at its peak value is $N_n = 0.197 \pm 0.020$. This should be compared with the normalization constant for the ^{3}He$(p, 2p)d$ PWIA cross sections ($N_n = 0.169 \pm 0.017$).

C. ^{3}He$(p, 2p)pn$

The $(p, 2p)$ continua corresponding to the breakup of ^{3}He into three nucleons are to a large extent structureless except for a pronounced ridge at the boundary. As discussed above, this pronounced ridge corresponds to the ^{3}He$(p, 2p)d^*$ reaction. A scatter plot representing a typical situation is shown in Fig. 10. After subtraction of the ^{3}He$(p, 2p)d^*$ contribution the continua were projected on the T_3 axis. Figure 11 shows the projected continua at 50°-40°, 40°-70°, and 40°-40°. The solid curves represent the differential phase space distribution[22] normalized to the experimental data in each case. The normalization constants agree within the relative error with which the continua were measured. There exist reasonable agreement between the phase space distributions and the projected spectra. Within the statistical accuracy of

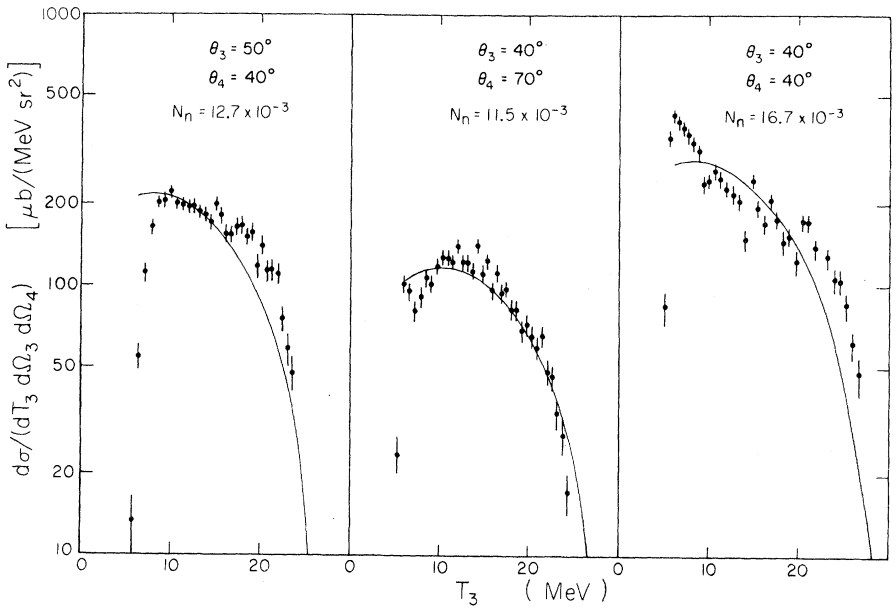

FIG. 11. Continua of the ^{3}He$(p, 2p)pn$ reaction at 50°-40°, 40°-70°, and 40°-40°. The contribution of the ^{3}He$(p, 2p)d^*$ reaction has been subtracted from the data. The solid curves represent the differential phase-space distributions normalized to the experimental result. The normalization constants are in units of μb/(MeV^{4}sr^2).

the data there is no indication of any structure which is consistent with the kinematic criteria for excited states of ^{3}He.[27] Quantitatively, the discrepancies between the differential phase-space distributions and the experimental continua are the same as or less than observed by Epstein *et al.*[28] The observed deviations occur in the corresponding regions of momentum space. The enhancement in the 50°-40° continuum near $T_3 = 22$ MeV is most likely due to quasifree scattering from a correlated n-p pair or a d^* configuration, i.e., the reaction $^3\mathrm{He}(p, pd^*)p$ with a proton as spectator. A similar enhancement has been found in the continua of the $^3\mathrm{H}(p, 2p)nn$ reaction at 45.6 MeV.[29]

In summary: (1) Within the framework of the PWIA, there exists reasonable agreement between the extracted momentum distributions for the $p+d$ and $p+d^*$ systems in ^{3}He and theoretical predictions calculated using relatively simple wave functions for ^{3}He, d, and d^*. (2) The momentum distribution extracted from the $^3\mathrm{He}(p, 2p)d$ energy-sharing data appears to be somewhat wider than the one extracted from the angular-correlation data indicating the need for further studies at higher incident energies. (3) The $^3\mathrm{He}(p, pd)p$ quasifree scattering peaks show marked distortions likely due to interference with the pseudo two-body process $p + {}^3\mathrm{He} \rightarrow d + [pp]$. The interference effects will slowly disappear with increasing incident proton energies provided not too small angles are chosen. (4) The normalizations of the PWIA predictions to experiment for the $^3\mathrm{He}(p, 2p)d$ and $^3\mathrm{He}(p, pd)p$ reactions are different at an incident proton energy of 45 MeV (0.169 as compared to 0.197). (5) The $^3\mathrm{He}(p, 2p)pn$ continua agree to a large extent with differential phase-space distributions.

The authors would like to thank Mark Sybe de Jong for his help with data reduction and analysis, and Dr. Daniel I. Bonbright for helpful discussions.

---

†Work supported in part by the Atomic Energy Control Board of Canada.

*Present address: Simulation Physics Corporation, Irvine, California 92707.

‡Present address: Department of Physics, Texas A&M University, College Station, Texas 77843.

§Present address: Nuclear Research Centre, University of Alberta, Edmonton, Alberta, T6G 2J1.

¶Present address: Department of Physics, University of Birmingham, Birmingham, England.

[1]G. Jacob and T. A. J. Maris, Rev. Mod. Phys. 38, 121 (1966); 45, 6 (1973).

[2]K. H. Bray, S. N. Bunker, M. Jain, K. S. Jayaraman, C. A. Miller, J. M. Nelson, W. T. H. van Oers, D. O. Wells, J. Janiszewski, and I. E. McCarthy, Phys. Lett. 35B, 41 (1971).

[3]D. R. Lehman, Phys. Rev. C 6, 2023 (1972); R. D. Haracz and T. K. Lim, Phys. Rev. C 9, 569 (1974).

[4]I. Šlaus, M. B. Epstein, G. Paić, J. R. Richardson, D. L. Shannon, J. W. Verba, H. H. Forster, C. C. Kim, D. Y. Park, and L. C. Welch, Phys. Rev. Lett. 27, 751 (1971).

[5]H. G. Pugh, P. G. Roos, A. A. Cowley, V. K. C. Cheng, and R. Woody, III, Phys. Lett. 46B, 192 (1973).

[6]R. Frascaria, V. Comparat, N. Marty, M. Morlet, A. Willis, and N. Willis, Nucl. Phys. A178, 307 (1971).

[7]P. Kitching, G. A. Moss, W. C. Olsen, W. J. Roberts, J. C. Alder, W. Dollhopf, W. J. Kossler, C. F. Perdrisat, D. R. Lehman, and J. R. Priest, Phys. Rev. C 6, 769 (1972).

[8]H. H. Forster, M. Furić, C. C. Kim, D. Y. Park, M. B. Epstein, J. R. Richardson, I. Šlaus, and J. W. Verba, in *Few Particle Problems in the Nuclear Interaction*, edited by I. Šlaus, S. A. Moszkowski, R. P. Haddock, and W. T. H. van Oers (North-Holland, Amsterdam, 1972), p. 624.

[9]A. A. Cowley, P. G. Roos, H. G. Pugh, V. K. C. Cheng, and R. Woody, III, Nucl. Phys. A220, 429 (1974).

[10]R. Frascaria, V. Comparat, N. Marty, M. Morlet, and A. Willis, in *Few Particle Problems in the Nuclear Interaction* (see Ref. 8), p. 628.

[11]M. B. Epstein, I. Šlaus, D. L. Shannon, H. H. Forster, M. Furić, C. C. Kim, and D. Y. Park, Nucl. Phys. A199, 225 (1973).

[12]M. B. Epstein, I. Šlaus, D. L. Shannon, J. R. Richardson, J. W. Verba, H. H. Forster, C. C. Kim, and D. Y. Park, Phys. Lett. 36B, 305 (1971).

[13]A preliminary account of some of the results of the present experiment has been presented previously: M. Jain, S. N. Bunker, C. A. Miller, J. M. Nelson, and W. T. H. van Oers, Nuovo Cimento Lett. 8, 844 (1973).

[14]E. S. Y. Tin, Ph.D. thesis, University of Manitoba, 1974 (unpublished).

[15]M. H. MacGregor, R. A. Arndt, and R. M. Wright, UCRL Report No. 50426, 1966 (unpublished).

[16]E. F. Redish, G. J. Stephenson, Jr., and G. M. Lerner, Phys. Rev. C 2, 1665 (1970).

[17]M. Jain, P. G. Roos, H. G. Pugh, and H. D. Holmgren, Nucl. Phys. A153, 49 (1970).

[18]J. W. Watson, H. G. Pugh, P. G. Roos, D. A. Goldberg, R. A. J. Riddle, and D. I. Bonbright, Nucl. Phys. A172, 513 (1971).

[19]J. C. Gunn and J. Irving, Phil. Mag. 42, 1353 (1951).

[20]M. J. Moravcsik, Nucl. Phys. 7, 113 (1958).

[21]C. F. Perdrisat, L. W. Swenson, P. C. Gugelot, E. T. Boschitz, W. K. Roberts, J. S. Vincent, and J. R. Priest, Phys. Rev. 187, 1201 (1975).

[22]W. T. H. van Oers, M. Jain, and S. N. Bunker, Nucl.

Instrum. Methods 112, 405 (1973).
[23]L. Hulthén and M. Sugawara, in *Handbuch der Physik*, edited by S. Flügge (Springer-Verlag, Berlin, 1957), Vol. 39, p. 106.
[24]C. Y. Hu, Phys. Rev. C 3, 2151 (1971).
[25]C. C. Chang, E. Bar-Avraham, H. H. Forster, C. C. Kim, P. Tomas, and J. W. Verba, Nucl. Phys. A136, 337 (1969).
[26]S. N. Bunker, J. M. Cameron, J. R. Richardson, W. T. H. van Oers, and J. W. Verba, Nucl. Phys. A113, 461 (1968).
[27]S. N. Bunker, M. Jain, C. A. Miller, J M. Nelson, P. J. Tivin, and W. T. H. van Oers, Can. J. Phys. 50, 1295 (1972).
[28]M. B. Epstein, I. Šlaus, D. L. Shannon, H. H. Forster, M. Furić, C. C. Kim, and D. Y. Park, Nucl. Phys. A199, 225 (1973).
[29]D. I. Bonbright, S. A. Elbakr, A. Houdayer, C. A. Miller, D. J. Roberts, E. S. Y. Tin, W. T. H. van Oers, and J. W. Watson, in *Few Body Problems in Nuclear and Particle Physics*, edited by B. Cujec and R. J. Slobodrian (to be published).